Simulation of coherent synchrotron radiation emission from rotating relativistic electron layers

Bjoern S. Schmekel*
Department of Physics, Cornell University, Ithaca, New York 14853, USA
(Received 3 March 2005; revised manuscript received 16 May 2005; published 23 August 2005)

The electromagnetic radiation of rotating relativistic electron layers is studied numerically using particle-in-cell simulation. This system is general enough to be applied to problems involving the coherent synchrotron radiation (CSR) instability in bunch compressors and possibly in radio pulsars where the CSR instability may be used to explain the high brightness temperature and the observed spectra. The results of the simulation confirm all relevant scaling properties predicted by theoretical models and suggest that their range of validity is bigger than conservative estimates indicate. This is important for radio pulsars where the allowed parameter range is unknown.

DOI: 10.1103/PhysRevE.72.026410 PACS number(s): 41.60.Ap, 41.75.Ht, 52.27.Jt, 52.27.Ny

Extremely high brightness temperatures encountered, for example, in the radio emission of pulsars cannot be explained by an incoherent radiation mechanism for which the radiated power is proportional to the number of radiating charges. However, if all outgoing waves interfere constructively, the total power scales as the square of that number. In future particle accelerators the wavelength of the emitted radiation can easily reach the length of the accelerated bunches such that bunches can modulate themselves by means of their own radiation. The possible energy loss caused by coherent synchrotron radiation (CSR) would be undesirable for the operation of such accelerators.

The aim of the present work is to test the results obtained from the model developed by Schmekel, Lovelace, and Wasserman [1] numerically and probe its range of validity. The model predicts growth rates, saturation amplitudes, and the emitted power for an initial perturbation of a rotating relativistic cylinder of charged particles in an external magnetic field. The linear instability is closely related to the instability found by Goldreich and Keeley [2]. More recently CSR has been investigated in the particle accelerator physics community—e.g., [3–6].

In [1] the distribution function is chosen such that the azimuthal canonical angular momentum is fixed and the energy drops off exponentially. For the time being all fields and distribution functions are assumed to be uniform in the z direction. The equilibrium can be parametrized by the radius r_0 of the cylinder, the relative energy spread $\delta E/E \equiv v_{th}^2$ of the particles, the Lorentz factor γ, and the dimensionless field reversal parameter

$$\zeta \equiv \frac{4\pi e n_0 v_\phi r_0 v_{th}\sqrt{\pi/2}}{B_z^{ext}}, \tag{1}$$

where n_0 is the central number density, v_ϕ the azimuthal velocity, B_z^{ext} is the external magnetic field in the z direction in cgs units, and $c=1$. Considering all perturbed quantities to have the dependence $\exp(im\phi - i\omega t + k_r r)$ one obtains for $m^{2/3} v_{th} \ll 1$, $k_r v_{th} r_0 \ll 1$ and $|\Delta\tilde{\omega}| \ll \gamma^{-2}$ the dispersion relation

$$1 = -i\pi\zeta J_m(\omega r_0) H_m(\omega r_0)\gamma^{-2}(\Delta\tilde{\omega})^{-2} F_0 \tag{2}$$

and the growth rate

$$\mathrm{Im}(\omega) \simeq \frac{1.083\zeta^{1/2} m^{2/3}\dot{\phi}}{\gamma}\sqrt{F_0}, \tag{3}$$

where $\Delta\tilde{\omega} = (\omega - m\dot{\phi})/(m\dot{\phi})$, $H_m = J_m + iY_m$ with the Bessel functions J_m and Y_m, $\dot{\phi}$ is the angular velocity, the overdot denotes the time derivative, and

$$F_0 \equiv \frac{1}{2\pi}\int_{-\pi}^{\pi} e^{-m^2 v_{th}^2 (1-\sin\theta)^2/2} d\theta. \tag{4}$$

The radiated power is given by

$$P_m \approx 3.71 \times 10^{14} \gamma^6 m^{-3} \frac{L}{r_0}\left(\frac{\mathrm{Im}(\omega)}{\dot{\phi}}\right)^4 \mathrm{erg/s}. \tag{5}$$

Here the length of the cylindrical layer is denoted by L. The quoted expression was derived by approximating Bessel functions with Airy functions. It was shown that this approximation is valid under the conditions $m \gg 1$ and $m \gg \zeta^{3/2}\gamma^3 \equiv m_1$. The used dispersion relation was derived under the assumption $|\Delta\tilde{\omega}| \ll \gamma^{-2}$ (which is approximately equivalent to $m \gg m_1$), but this condition may be too strict. There is evidence that this is indeed the case, and one objective of this article is to confirm this. Especially for the study of radio pulsars bigger growth rates may be necessary to explain the observed brightness temperature.

For the simulation the software package OOPIC [7] was used. OOPIC is a relativistic two-dimensional particle-in-cell code which supports both plain (x,y) geometries and cylindrical (r,z) geometries. Since the interesting dynamics takes places in the azimuthal direction, one can only simulate a thin ring (instead of a cylinder) in the (x,y) mode. Loading the initial circular particle distribution in the (x,y) mode required modifying the source code (files load.cpp, diagn.cpp and c_utils.c) to allow the program to handle circular particle distributions. Some minor modifications were necessary in order to compile XOOPIC-2.5.1 with gcc 3.2.2 and the compiler compiler bison 1.28 under SunOS 5.9. The built-in function parser was extended to support elliptic integrals.

*Electronic address: bss28@cornell.edu

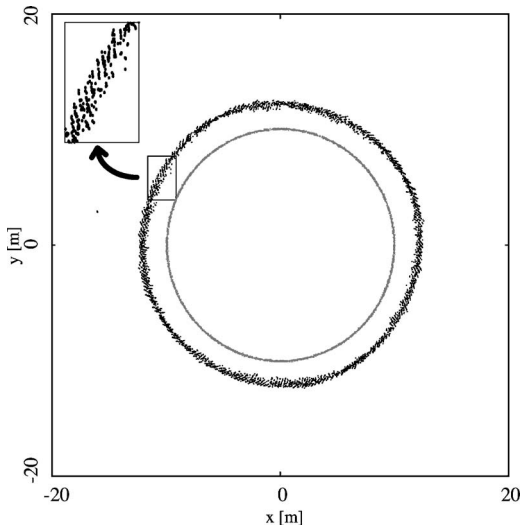

FIG. 1. Initial particle distribution (gray) and the same distribution after 23 ns have elapsed. Parameters: $\zeta=0.010$, $\gamma=30$, and $v_{th}=0.002$.

Since a thin ring of particles is simulated instead of a cylinder thereof all fields and charges were divided by the length L of the cylinder whereas the electron mass needs to be divided by L^2. $L=10r_0$ is chosen unless noted otherwise. The electric and magnetic self-fields for a thin ring equilibrium differ from what was used in the model. The fields can be found in [8]. It is ensured that OOPIC uses these self-fields before the perturbation starts to build up. As it turns out, choosing the correct self-fields is not too crucial. Leaving them out the system will build them up itself. Once the self-fields are created, the system shows no difference in behavior. The absence of the self-fields in the dispersion relation might help to understand this feature. As in [1] a Gaussian number density profile with rms width v_{th} was chosen for the initial distribution. Here 5000 macroparticles were tracked on a grid with resolution 512×512 unless noted otherwise. Once an energy for a particle has been chosen, it is placed at the equilibrium radius $r_0=m\gamma c(eB)^{-1}$; i.e., neglecting betatron oscillations, particles on the same orbit have the same energy. This determines the azimuthal component of the angular momentum. The system can pick up transverse motion quickly. The grid represents a rectangular region 40 m$\times$40 m big where the ring with radius $r_0=10$ m is centered.

In Fig. 1 the initial particle distribution (gray) and the particle distribution after 23 ns are shown. The parameters are $\zeta=0.010$, $\gamma=30$, and $v_{th}=0.002$. Qualitatively, a bunching of the particle distribution can be observed. An enlargement of a small section of Fig. 1 is also shown in the same figure. In Fig. 2, the bunching is shown for successively higher energy spreads. With increasing energy spread the bunches become fuzzier and the clean gaps between bunches that can be observed for small energy spreads are populated with "stray particles." This suggests that it may be harder to achieve complete coherence for larger values of v_{th}. The decoherence due to the nonzero width of the particle beam is investigated quantitatively later in the paper. These qualitative features are independent of γ.

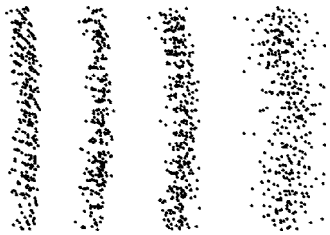

FIG. 2. Particle distribution ($\gamma=30$, $\zeta=0.01$) after 23 ns for $v_{th}=0.002$, $v_{th}=0.008$, $v_{th}=0.015$, and $v_{th}=0.033$ (from left to right). The four figures depict an approximately 6.5 m long segment.

Also note that during the evolution of the circular charge distribution both the radius and the width of the ring increase slightly. The former is due to (a) particles losing energy and (b) the perturbed magnetic field changing significantly. It tends to decrease for small energy spreads and increase for larger energy spreads. Starting with a larger radius the radius increases even further; i.e., this is not a relaxation from a "false" to a true equilibrium. Since the nonzero mesh size imposes an upper limit on the azimuthal mode number m which can become unstable, it is expected that the distance between bunches decreases as the resolution increases. This is indeed the case. For larger energy spreads the bunching of the distribution becomes hardly visible, but it still can be observed in the z component of the magnetic field (Fig. 3).

The bunches are slightly tilted and may be connected by a very thin inner ring of particles for sufficiently high beam currents. For these reasons it is not possible to Fourier transform the charge perturbations in order to compute the growth rates for each value of m. Since the resolutions used were low, the range of m values is restricted. Therefore, only the

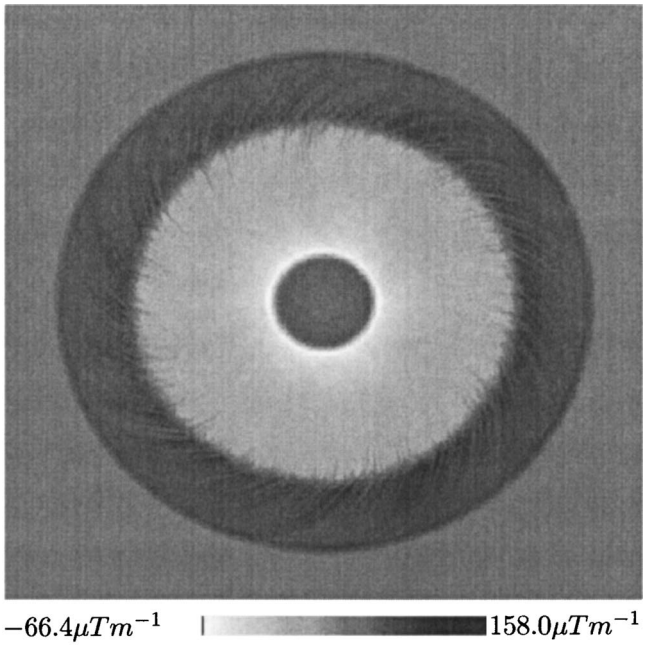

FIG. 3. z component of the magnetic field (self-field plus perturbation without external magnetic field) after 23 ns for $\zeta=0.010$, $\gamma=30$, and $v_{th}=0.025$. The size of the area depicted is 40 m$\times$40 m.

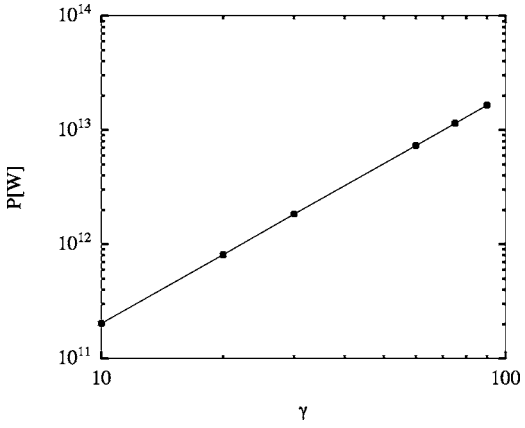

FIG. 4. Loss of kinetic energy in W vs γ for $\zeta=0.01$ and $v_{th}=0.002$.

radiated power is computed which can be obtained easily. Estimates of the growth rate are 2 orders of magnitude higher than what would be expected. A possible explanation is that the ratio between the saturation amplitude and the electric self-field,

$$\left|\frac{\delta E_{sat}}{E_{self}}\right| = \frac{1}{m\zeta}\left(\frac{\mathrm{Im}(\omega)(m)}{\dot{\phi}}\right)^2, \tag{6}$$

is typically of the order of 10^{-3} for the given sample cases which is rather small. The initial perturbations due to discreteness, numerical noise, etc., are usually in the same order of magnitude. Therefore, one cannot expect to see the regime covered by the linearized Vlasov equation. This is another reason for focusing entirely on the emitted power.

In Figs. 4 and 5 the radiated power determined by measuring the kinetic energy loss of the electron cloud after approximately 2.36 ns is plotted as a function of γ and ζ, respectively. After 0.24 ns the perturbations have saturated and the emitted power is fairly constant. A quadratic dependence

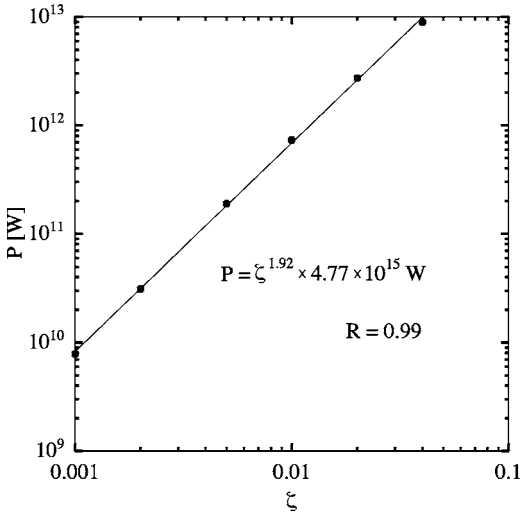

FIG. 5. Loss of kinetic energy in W vs ζ for $\gamma=30$ and $v_{th}=0.025$. The solid line shows the best fit.

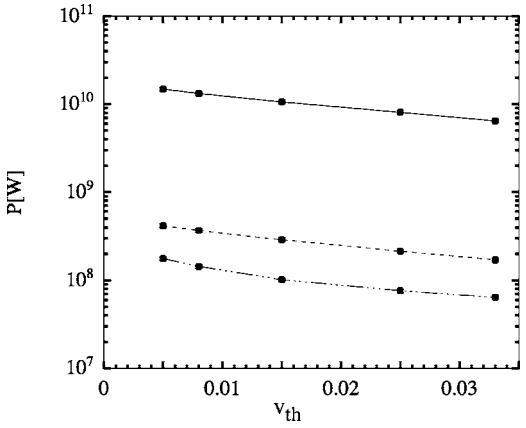

FIG. 6. Total power radiated as obtained from OOPIC for the parameters $\zeta=0.01$, $\gamma=30$ (solid line) and $\zeta=0.005$, $\gamma=10$ (dashed line). The dash-dotted line is proportional to $\Sigma_{m=1}^{\infty}P_m$.

can be established; i.e., the first two relevant scalings expected from the analytical model are recovered.

The simulation has been repeated at lower (256×256) and higher (1024×1024) resolution. No significant effect could be observed. This is consistent with the model which predicts that most power is emitted by modes with low m. The resolution is not high enough to resolve the path length difference of orbits with different radii at these low values of v_{th}. Also, decreasing the step size dt to 2.5 ps and increasing the number of macroparticles to 50 000 has a negligible effect.

Finally, the effect of the energy spread is investigated. With increasing v_{th} the power decreases which is due to the decoherence described by the factor F_0 defined in Eq. (4). The results are plotted in Fig. 6 for the parameters $\zeta=0.01$, $\gamma=30$ and $\zeta=0.005$, $\gamma=10$, respectively, and $L=r_0$. In the former case m_1 is 27, and in the latter case it is 0.4. Equation (5) becomes

$$P \approx (3.71\times10^{14}\ \mathrm{erg/s})\frac{L}{r_0}\gamma^2\sum_m m[i\pi J_m(\omega r_0)H_m(\omega r_0)]^2. \tag{7}$$

Despite m_1 being much larger than 1, for the first set of parameters the slopes in Fig. 6 match exactly only if the summation starts at $m=1$. This suggests that modes with $m<m_1$ do radiate and can be described by the same dispersion relation. Since the power scales as $m^{-5/3}$, these modes may actually be very important for computing the total energy loss. Note that while the simulation suggest $P\propto L^2$, Eq. (5) (which was derived under the assumption $L\gtrsim r_0$) gives $P\propto L$. A two-dimensional simulation cannot explain how the radiation from different axial positions on the cylinder interacts. In the thin ring case doubling L doubles the number of particles, N, and therefore quadruples P. Fortunately, as can be seen in the derivation of Eq. (5) in [1] the ζ-, v_{th}- and γ-dependent part of P is independent of L. In Fig. 6 the overall factor matches if $r_0=100L$ whereas the growth rate for a perturbation of a cylinder and a thin ring coincide for $r_0=L$ [1]. Also note that Fig. 1 suggests $k_r v_{th} r_0 \sim 1$, whereas

Eq. (3) was derived under the assumption $k_r v_{th} r_0 \ll 1$.

The particle in cell code OOPIC was used to simulate the evolution of density perturbations in a thin ring of charged particles which move in relativistic almost circular motion in an external magnetic field. The results were compared with the model in [1]. Comparisons of the simulation with the model show approximate agreement with the main predicted scaling relations. In particular the bunching effect could be observed very clearly and the emitted power is proportional to the square on the number density which implies coherent radiation. The dependence on the energy spread can be recovered exactly assuming all modes contribute to the observed energy loss, suggesting that the model may apply even if $m < m_1$.

I thank Richard V. E. Lovelace, Georg H. Hoffstaetter, Ira M. Wasserman, and Joseph T. Rogers for valuable discussions and John P. Verboncoeur for his help with OOPIC. This research was supported by the Stewardship Sciences Academic Alliances program of the National Nuclear Security Administration under U.S. Department of Energy Cooperative Agreement No. DE-FC03-02NA00057.

[1] B. S. Schmekel, R. V. E. Lovelace, and I. M. Wasserman, Phys. Rev. E **71**, 046502 (2005).
[2] P. Goldreich and D. A. Keeley, Astrophys. J. **170**, 463 (1971).
[3] G. Stupakov and S. Heifets, Phys. Rev. ST Accel. Beams **5**, 054402 (2002).
[4] S. Heifets, S. Krinsky, and G. Stupakov, SLAC Report No. SLAC-PUB-9165 (2005).
[5] F. Sannibale *et al.*, in *Proceedings of the 2003 Particle Accelerator Conference, Portland, Oregon, 2003*, edited by J. Chew, P. Lucas, and S. Webber (IEEE, Piscataway, NJ, 2003).
[6] M. Venturini, R. Warnock, R. Ruth, and J. A. Ellison, Phys. Rev. ST Accel. Beams **8**, 014202 (2005).
[7] J. P. Verboncoeur, A. B. Langdon, and N. T. Gladd, Comput. Phys. Commun. **87**, 199 (1995).
[8] J. D. Jackson, *Classical Electrodynamics* (Wiley, New York, 1998).